

Inertia tensor estimation for a rigid nadir pointing satellite based on star tracker

Mohammed E. A. Cheriet^a, Abdellatif Bellar^{*}, Mohammed Y. Ghaffour^b,
Akram Adnane^c and Mohammed A. SI Mohammed^d

*Department of Space Mechanics Research, Satellite Development Center,
BP 4065 Ibn Rochd USTO, Oran, Algeria*

(Received September 2, 2020, Revised February 24, 2021, Accepted March 4, 2021)

Abstract. Accurate inertia properties information is important to reach an optimized estimation of attitude and precise control of a rigid spacecraft. Unfortunately, the satellite is succumbing several influences that can affect the inertia properties, such as fuel consumption and sloshing. Thus, this work inspects the use of star tracker to estimate the attitude, angular velocity and moment of inertia for a rigid nadir pointing satellite by employing extended Kalman filter, without any prior information about the nominal inertia matrix. The proposed estimator is applied in nadir pointing mode and without any constant control torque to avoid the attitude tumbling during the estimation phase, which in turn leads to a catastrophic failure of the satellite mission. The simulation results are compared to three other approaches and validated by Monte Carlo method that elucidates the good performance of the suggested approach and demonstrates its efficiency in satellite inertia tensor and attitude estimation even in worst situations.

Keywords: extended Kalman filter; inertia tensor; satellite; star tracker

1. Introduction

Accurate control of a satellite certainly requires a correct estimate of its mass property including inertia matrix, which changes over time under the influence of various factors such as fuel consumption, slosh, deployment of the appendages, and so on.

The inertia property estimation is more efficient when performed in orbit, using the on-board sensors, and applying optimal estimation methods. However, the problem of mass property estimation is a challenging subject that attracted the attention of loads of researchers in recent years, and several methods have been proposed for different kinds of satellites.

Several least squares based algorithms have been adopted for inertia tensor estimation. Kutlu *et al.* (2007) estimated the Moment of Inertia (MOI) values for LEO satellite using Least Square Estimation (LSE) using gyroscopes, magnetometer and sun sensor data. Palimaka and Burlton

*Corresponding author, Ph.D., E-mail: abellar@cds.asal.dz

^aPh.D., E-mail: mcheriet@cds.asal.dz

^bSenior Engineer, E-mail: myghaffour@cds.asal.dz

^cPh.D., E-mail: aadnane@cds.asal.dz

^dProfessor, E-mail: masimohammed@cds.asal.dz

(1992) focused his effort toward the estimation of on-orbit data with the application of a gyostat model attitude dynamics integrator. As a result, weighted-least-squares (WLS) process has been applied regardless of the solutions of equations of motion and derivatives. Tanygin and Williams (1997) considered the problem of estimating the mass property of a spinning rigid body and adopted the parameter estimation method, which allows determining both the inertia matrix and the body centre of mass. The inertia was estimated using coasting manoeuvres. A recursive least squares (RLS) procedure for use in orbit has been used by Bordany *et al.* (2000) to estimate the inertia property. Keim *et al.* (2006) formulated the problem of inertia estimation based on a constraint least squares (LS) minimization problem where the inertia matrix is explicitly constrained and incorporated as linear matrix inequalities. Chashmi and Malaek (2016) developed a new modular formulation to simultaneously determine inertia parameters of an autonomous space robot while it captures a target space object. This approach is based on RLS algorithm, and it is appropriate for simultaneous estimation processes. The simulation of extensive case studies reveals that time is significantly reduced. Lorenzetti *et al.* (2017) determined the products of inertia for small scale unmanned Aerial Vehicles (UAVs) using a mathematical approach based on LS error minimization and knowing the angle between the aircraft X-body axis and principal X-axis. Therefore, this technique was applied to small UAV at NASA Armstrong Flight Research Centre. According to the author's, the main limitation of this method is the need of the test rig which could be difficult to apply for some large or heavy vehicles. Zhai *et al.* (2017) proposed a new method to design and calculate the optimal excitation to improve the identification of spacecraft inertia parameters using the LS method. Simulation results show that this method has a good performance index and can enhance the identification of inertia property. Xu and Wang (2017) estimated the inertia parameters of a free-flying space object using an algorithm based on vision and the LS method. The author has used a bullet to excite the space object in order to enhance the amount of pertinent information. Simulation results illustrate that his algorithm is practical to estimate the moment of inertia (MOI) of free fly space object.

Being widely used in estimation problems, the Kalman filter (KF) is present in many works related to mass property, Bergmann *et al.* (1987) developed real time algorithms that estimate mass properties based upon stochastic estimation. Inverse inertia matrix and the center of mass, were estimated by a second-order filter from noisy measurements of the angular velocity, while KF was used to estimate the mass reciprocal. Its simulation results show that the mass properties were estimated with an error around 1%. Zhao *et al.* (2009) applied the KF to estimate, online, the mass property of mated spacecraft using an optimal approach based on excitation torques, measurements of attitude control and momentum management. Linares *et al.* (2012) inspected the problem of estimating the inertia property of a space object using photometric and astrometric data with an Unscented Kalman Filter (UKF). A new real time method for estimating the inertia property has been suggested by Yang *et al.* (2015). They used the extended Kalman filter (EKF) to reduce the gyro noise and RLS algorithm to estimate the inertia properties. Yoon *et al.* (2017) estimated the MOI and different parameters of attitude for a nanosatellite using the new Kalman filter formulation based on the differential form of the rigid-body rotational dynamics and different attitude parameters, excluding gyroscope information. The algorithm is endorsed by exploiting three different types of unmodelled disturbance torques. The simulation results of this method are especially practical for nanosatellite applications in which gyroscope measurements are imprecise. An estimation method by reformulating Euler equations of motion is suggested to obtain a regressor matrix. Then, the EKF and linear LS are used to reduce the gyros noise and estimate the inertia property (Kim *et al.* 2010, 2016). Reliable and accurate angular accelerations were

achieved when using a Savitzky-Golay filter based on an even number sampled data. Recently, Bellar has proposed an algorithm to estimate the moment of inertia and angular velocity based on EKF through gyroscope measurement and without using any nominal inertia matrix (Bellar and Mohammed 2019).

Besides, Bergmann and Dzielski (1990) considered a rigid spacecraft and used only torque-producing estimation in developing its algorithm for mass properties estimation, which prevents fuel usage, disturbances and contamination issues associated with the use of reaction control for identification of mass properties. Thienel *et al.* (2008) proposed an adaptively method to estimate the six inertia parameters of a rigid spacecraft as part of a passivity based on a nonlinear passivity adaptive control scheme. The method was validated by two sample simulations that demonstrate the estimation for both different sizes of spacecraft.

The spacecraft inertia tensor has been estimated on orbit by Manchester using a recursive algorithm based on semi definite programming (SDP). The interesting point of this technique is the availability of fast numerical solvers for SDPs which makes it convenient for off-line analysis and real-time implementation (Manchester and Peck 2017). Ni *et al.* (2017) ameliorated the recursive predictor-based subspace identification to identify the MOI parameters of on-orbit spacecraft. The approach has been validated by comparing it with the classical subspace method based on the singular value decomposition. The simulation results show that his algorithm is better and can be exploited to determine the MOI parameters effectively. Muliadi *et al.* (2017) proposed the ARES method to determine UAV's MOI simultaneously. This method is based on the UAV flight data to accommodate accuracy issues of modelling. The implementation of ARES method in the quadrotor flight data shows that ARES successfully measured the asymmetrical terms which is important for nonlinear control.

With a similar motivation to the above-mentioned authors, we mainly contribute to existing knowledge on the estimation of inertia property by:

- Introducing a star tracker, which provides higher attitude accuracy in comparison with the other sensors of attitude determination and control system.
- Bypassing the application of a torque that may be harmful to the stability of our system, by coming up with a suitable approach to the nominal mode of our rigid spacecraft.
- Improving the angular velocity estimation using the estimated inertia matrix rather than the nominal one.
- Estimating the full attitude and inertia tensor, based on the star tracker data, with an EKF algorithm, randomly initialized.

The proposed approach presents the advantage of full attitude estimation together with the moment of inertia from the star tracker data, with no need of a nominal inertia matrix that has an unfavourable effect on the angular velocity estimation. Moreover, the method allows us to avoid the application of constant control torques that put the satellite in undesirable tumbling attitude and cause angular velocity divergence.

This paper begins by modelling the satellite dynamics and kinematics. It will then go on to the control law using error quaternions. Then, the EKF algorithm and sensor measurements model will be formulated. After that, the simulation results illustrate the performance of the proposed approach where the Monte Carlo method is used to validate them. Finally, the conclusion gives a brief summary of the findings.

2. Estimation and control design

This section presents the theoretical part of attitude dynamics and kinematics, control Law and

estimator design.

2.1 Attitude dynamics and kinematics

The angular momentum of a three axis reaction wheels satellite, is given by (Wertz 2012, Bellar and Mohammed 2019)

$$J\dot{\omega}_B^I = -\omega_B^I \times (J\omega_B^I + h) - \dot{h} + T_d \quad (1)$$

where $\omega_B^I = [\omega_x \ \omega_y \ \omega_z]^T$ is the angular velocity vector in the inertial frame;

$J = \text{diag}[I_{xx} \ I_{yy} \ I_{zz}]$ is the inertia matrix of satellite;

$T_d = [T_{dx} \ T_{dy} \ T_{dz}]$ is the external disturbance torque vector;

$h = [h_x \ h_y \ h_z]$ is the reaction wheels angular momentum vector;

$\dot{h} = [\dot{h}_x \ \dot{h}_y \ \dot{h}_z]$ is the applied torque vector by 3-axis reaction wheels.

To avoid the singularities and trigonometric functions, the Euler symmetric parameters (quaternions) are used to represent the satellite attitude. The following differential equation propagates the quaternion kinematic (Wertz 2012, Yang and Zhou 2017, Yadegari et al. 2018)

$$\dot{q} = \frac{1}{2} \Omega q \quad (2)$$

$$\Omega = \begin{bmatrix} 0 & \omega_{oz} & -\omega_{oy} & \omega_{ox} \\ -\omega_{oz} & 0 & \omega_{ox} & \omega_{oy} \\ \omega_{oy} & -\omega_{ox} & 0 & \omega_{oz} \\ -\omega_{ox} & -\omega_{oy} & -\omega_{oz} & 0 \end{bmatrix} \quad (3)$$

where $q = [q_1 \ q_2 \ q_3 \ q_4]^T$ is the attitude quaternion vector;

$\omega_B^o = [\omega_x \ \omega_y \ \omega_z]^T$ is the orbit-referenced angular body rate vector;

The attitude transformation matrix of any vector from the reference orbital to body coordinate in terms of quaternions is expressed as follows (Wertz 2012, Adnane et al. 2018)

$$A = \begin{bmatrix} q_1^2 - q_2^2 - q_3^2 + q_4^2 & 2(q_1q_2 + q_3q_4) & 2(q_1q_3 - q_2q_4) \\ 2(q_1q_2 - q_3q_4) & -q_1^2 + q_2^2 - q_3^2 + q_4^2 & 2(q_2q_3 - q_1q_4) \\ 2(q_1q_3 - q_2q_4) & 2(q_2q_3 - q_1q_4) & -q_1^2 - q_2^2 + q_3^2 + q_4^2 \end{bmatrix} \quad (4)$$

The error quaternion represents the difference between the current and commanded quaternions as follows Sidi (1997)

$$\begin{bmatrix} q_{1e} \\ q_{2e} \\ q_{3e} \\ q_{4e} \end{bmatrix} = \begin{bmatrix} q_{4c} & q_{3c} & -q_{2c} & -q_{1c} \\ -q_{3c} & q_{4c} & q_{1c} & -q_{2c} \\ q_{2c} & -q_{1c} & q_{4c} & -q_{3c} \\ q_{1c} & q_{2c} & q_{3c} & q_{4c} \end{bmatrix} \quad (5)$$

where q_{ie} is the error quaternion vector; q_{ic} is the commanded quaternion vector.

2.2 Control law

A state control law uses error quaternions as attitude errors in three quaternion feedback control law. The closed loop Liapunov stability for 3-axis attitude manoeuvres has been demonstrated in

Wie *et al.* (1989). The control law is

$$\dot{h} = -Kq_{vec} - D\omega_B^I \quad (6)$$

where $q_{vec} = [q_{1e} \ q_{2e} \ q_{3e}]^T$ is the vector part of error quaternion;
 $K = diag[k_1 \ k_2 \ k_3]$ is the positive angular control gains for each axis;
 $D = diag[d_1 \ d_2 \ d_3]$ is the positive rate control gains for each axis;

When the commanded and the current quaternions coincide, the error quaternion $q_e = [0 \ 0 \ 0 \ 1]^T$.

2.3 Estimator design

In this section, the various steps of the design and the implementation of the proposed full state filter are performed. Explicit expressions of the system equation, transition matrix and observed equation are developed. Therefore, we present a more algorithm description omitting some theoretical considerations. It is worthy to mention that the basic theoretical concepts and the mathematical models of KF are described in detail in Yoon *et al.* (2017) and Zhai *et al.* (2017).

The state vector (10 elements), to be estimated, includes the inertial angular rate (ω_B^I), the attitude quaternion vector (q), and the MOI (J_m). The full state vector can be represented as

$$x = [\omega_B^I \ q \ J_m]^T = [\omega_x \ \omega_y \ \omega_z \ q_1 \ q_2 \ q_3 \ q_4 \ I_{xx} \ I_{yy} \ I_{zz}]^T \quad (7)$$

The dynamics and the kinematic model of the spacecraft can be expressed in vector form as follows

$$\begin{bmatrix} \dot{\omega}_B^I \\ \dot{q} \\ \dot{J}_m \end{bmatrix} = \begin{bmatrix} J^{-1} [-\omega_B^I \times (J\omega_B^I + h) - \dot{h} + T_{gg}] \\ \frac{1}{2} \Omega \ q \\ -\frac{1}{\tau} [I_{3 \times 3}] J_m \end{bmatrix} + \begin{bmatrix} u_\omega \\ 0_{4 \times 1} \\ 0_{3 \times 1} \end{bmatrix} \quad (8)$$

where I , τ , u_ω and T_{gg} are, respectively, the identity matrix, the time constant of the MOI, the white Gaussian noise with zero mean and gravity-gradient torque vector.

The following equation gives the non-linear model and the state equation

$$\frac{d}{dt}x(t) = f\{x(t), t\} + w(t) \quad (9)$$

where $w(t)$ is the state noise vector with zero mean and covariance $Q(t)$.

The EKF algorithm is set as follows

2.3.1 Propagation state

To propagate the state equation (Eq. (9)), we use the backward difference as

$$\hat{x}_{k+1/k} = \hat{x}_{k/k} + \hat{\dot{x}}_{k/k} \Delta t \quad (10)$$

where Δt is the integration step size.

The covariance propagation is

$$P_{k+1/k} = \Phi_{k+1/k} P_{k/k} \Phi_{k+1/k}^T + Q_{k+1} \quad (11)$$

where Q is the process noise covariance matrix and Φ is the state transformation matrix given by

$$\Phi_{k+1/k} \approx I_{10 \times 10} + F_{k+1/k} T_s \quad (12)$$

$$F_{k+1/k} = \begin{bmatrix} \frac{\partial \dot{\omega}_B^I}{\partial \omega_B^I} & \frac{\partial \dot{\omega}_B^I}{\partial q} & \frac{\partial \dot{\omega}_B^I}{\partial J_m} \\ \frac{\partial \dot{q}}{\partial \omega_B^I} & \frac{\partial \dot{q}}{\partial q} & \frac{\partial \dot{q}}{\partial J_m} \\ \frac{\partial \dot{J}_m}{\partial \omega_B^I} & \frac{\partial \dot{J}_m}{\partial q} & \frac{\partial \dot{J}_m}{\partial J_m} \end{bmatrix} \quad (13)$$

$$F_{k+1/k} = \begin{bmatrix} F_{3 \times 3}^{\omega\omega} & 0_{3 \times 4} & F_{3 \times 3}^{\omega J_m} \\ F_{4 \times 3}^{q\omega} & F_{4 \times 4}^{qq} & 0_{4 \times 3} \\ 0_{3 \times 3} & 0_{3 \times 4} & -\frac{1}{\tau} [I_{3 \times 3}] \end{bmatrix} \quad (14)$$

The process noise covariance matrix Q is defined as follows (Yoon *et al.* 2017, Zhai *et al.* 2017)

$$Q_k = \iint_k^{k+1} \Phi(t_{k+1}, u) E[w(u)w^T(v)] \Phi^T(t_{k+1}, v) du dv \quad (15)$$

where u and v are independent variables; for our application, it is assumed that only the angular velocity terms have process noise and the matrix E of dimension (10×10) is

$$E[w(u)w^T(v)] = \begin{bmatrix} E_{11} & 0_{3 \times 4} & 0_{3 \times 3} \\ 0_{4 \times 3} & 0_{4 \times 4} & 0_{4 \times 3} \\ 0_{3 \times 3} & 0_{3 \times 4} & 0_{3 \times 3} \end{bmatrix} \quad (16)$$

where

$$E_{11} = \text{diag}[s_1 \delta(u - v) \quad s_2 \delta(u - v) \quad s_3 \delta(u - v)] \quad (17)$$

δ is the Dirac Delta function and s is the spectral amplitude for angular velocity.

In Eq. (15), the term $\Phi(\Delta t, u) E[w(u)w^T(v)] \Phi^T(\Delta t, v)$ is computed as

$$\begin{bmatrix} (I_{3 \times 3} + F_{3 \times 3}^{\omega\omega} u) E_{11} (I_{3 \times 3} + F_{3 \times 3}^{\omega\omega} v)^T & 0_{3 \times 4} & (I_{3 \times 3} + F_{3 \times 3}^{\omega J_m} u) E_{11} (I_{3 \times 3} + F_{3 \times 3}^{\omega J_m} v)^T \\ F_{4 \times 3}^{q\omega} u E_{11} (I_{3 \times 3} + F_{3 \times 3}^{\omega\omega} v)^T & 0_{4 \times 4} & F_{4 \times 3}^{q\omega} u E_{11} (I_{3 \times 3} + F_{3 \times 3}^{\omega J_m} v)^T \\ 0_{3 \times 3} & 0_{3 \times 4} & 0_{3 \times 3} \end{bmatrix} \quad (18)$$

2.3.2 Correction state Observation Matrix

$$H_{k+1} = \begin{bmatrix} \frac{\partial z}{\partial \omega_B^I} & \frac{\partial z}{\partial q} & \frac{\partial z}{\partial J_m} \end{bmatrix} \quad (19)$$

where z is the quaternion measurement from the star tracker and the mathematical model of the sensor is

$$z = q + \eta \quad (20)$$

where η is the zero mean Gaussian white noise with covariance matrix R of the true quaternion of the satellite (q). The computed observation matrix is

$$H_{k+1} = [0_{4 \times 3} \quad I_{4 \times 4} \quad 0_{4 \times 3}] \quad (21)$$

Kalman Gain Matrix

$$K_{k+1} = P_{k+1/k} H_{k+1}^T (H_{k+1} P_{k+1/k} H_{k+1}^T + R_{k+1})^{-1} \quad (22)$$

Update state

$$\hat{x}_{k+1/k+1} = \hat{x}_{k+1/k} + K_{k+1}(z - H\hat{x}_{k+1/k}) \quad (23)$$

Update covariance

$$P_{k+1/k+1} = [I_{10 \times 10} - K_{k+1} H_{k+1}] P_{k+1/k} \quad (24)$$

3. Results and discussion

Aiming to show the advantages of our proposed approach, the simulation is performed in the following order:

- Establish an Orbit /Attitude propagator, which models the rigid microsatellite dynamics and kinematics over a period of 600 s based on the satellite parameters as summarized in Table 1. This propagator may include gravity gradient and aerodynamic drag as external perturbing torques.

- Apply a proportional derivative (PD) controller on a reaction wheels triad in a standard configuration. The controller is adopted for its simplicity, global stability and board applicability (Salem and Aly 2015). Knowing that the use of other controllers such as proportional–integral–derivative, sliding mode and H-infinity can also achieve three-axis attitude stabilization. The reaction wheel is characterized by a momentum of inertia equal to $8 \times 10^{-4} \text{ kg.m}^2$ and a maximum speed of $\pm 5000 \text{ rpm}$, which give a maximum angular momentum of 0.42 Nms and a maximum wheel torque of $5 \times 10^{-3} \text{ Nm}$.

- Design and implementation of an EKF algorithm to estimate the 10 elements of the state vector (angular velocity, quaternion and inertia tensor) based on the data provided by the star tracker. The estimator is randomly initialized and there is no need to use nominal inertia. Furthermore, the estimation is applied in nadir pointing mode.

- Table 2 summarizes the EKF parameters.

- Perform a static simulation through Monte-Carlo algorithm iterated 10000 times, within which the true inertia matrix change randomly over $\pm(0 \div 25)\%$ interval for each axis. The error between the estimated and the true inertia tensors is calculated at each iteration.

The estimated and the true angular velocities in three axes, as well as the error, are shown in Figs 1-2, respectively. The root mean square (RMS) error of the angular velocity estimation is about $2.8 \times 10^{-5} \text{ deg/s}$. Fig. 3 illustrates the real and estimated quaternion and quaternion estimation error, with an RMS approximately equal to 11.7×10^{-6} . Fig. 4 shows the estimated

Table 1 Propagator parameters

Parameters		Value
Orbital parameters	Inclination (<i>deg</i>)	98
	Initial ω (<i>deg/s</i>)	$[0 \ -0.06 \ 0]^T$
	Altitude (<i>km</i>)	700
Initial quaternion attitude		$[0.02571 \ -0.02662 \ 0.01813 \ 0.9992]^T$
Reference quaternion attitude		$[0 \ 0 \ 0 \ 1]^T$
Sample time (<i>s</i>)		0.1
True inertia tensor (<i>kg.m²</i>)		$[20.3 \ 17.3 \ 15.2]^T$

Table 2 Estimator parameters

Parameters		Value
Initial ω (<i>deg/s</i>)		$[0 \ -0.06 \ 0]^T$
Initial quaternion attitude		$[0 \ 0 \ 0 \ 1]^T$
Initial inertia tensor (<i>kg.m²</i>)		$[25 \ 20 \ 13]^T$
Measurement noise covariance matrix of star tracker R (σ)		3.2×10^{-5}
Time constant τ		10^6

Table 3 Performance comparison of algorithms

	LSE#1 Kutlu <i>et al.</i> (2007)	EKF#1 Kim <i>et al.</i> (2016)	EKF#2 Bellar and Mohammed (2019)	Proposed algorithm
Sensors	Gyroscope Magnetometer Sun sensor	Gyroscope	Gyroscope	Star Tracker
True inertia $[I_{xx} \ I_{yy} \ I_{zz}]$	[20 17 15]	[14.2 17.3 20.3]	[14.2 17.3 20.3]	[20.3 17.3 15.2]
Inertia estimation error (%)	[1.62 1.99 1.57]	[0.12 0.07 0.07]	[0.06 0.02 0.008]	[0.04 0.09 0.06]
Applied torque (<i>Nm</i>)	–	$[1 \ 1 \ -2] \times 10^{-3}$	$[1 \ 1 \ -2] \times 10^{-3}$	PD (nadir pointing mode)
Quaternion estimation error	0.02	–	–	11.7×10^{-6}
Angular velocity estimation error (<i>deg/s</i>)	0.2	5×10^{-3}	3.6×10^{-3}	2.8×10^{-5}
Validation test	–	–	Monte Carlo	Monte Carlo

and the true inertia tensors. The convergence time of the estimated inertia tensor is about 150 second.

Table 3 presents comparison between the proposed algorithm and three other methods implemented in Kutlu *et al.* (2007), Kim *et al.* (2016) and Bellar and Mohammed (2019). This comparison takes into account the quaternion, angular velocity and inertia tensor estimation error and the applied torque by reaction wheels. For simplification, these estimators are named LSE#1,

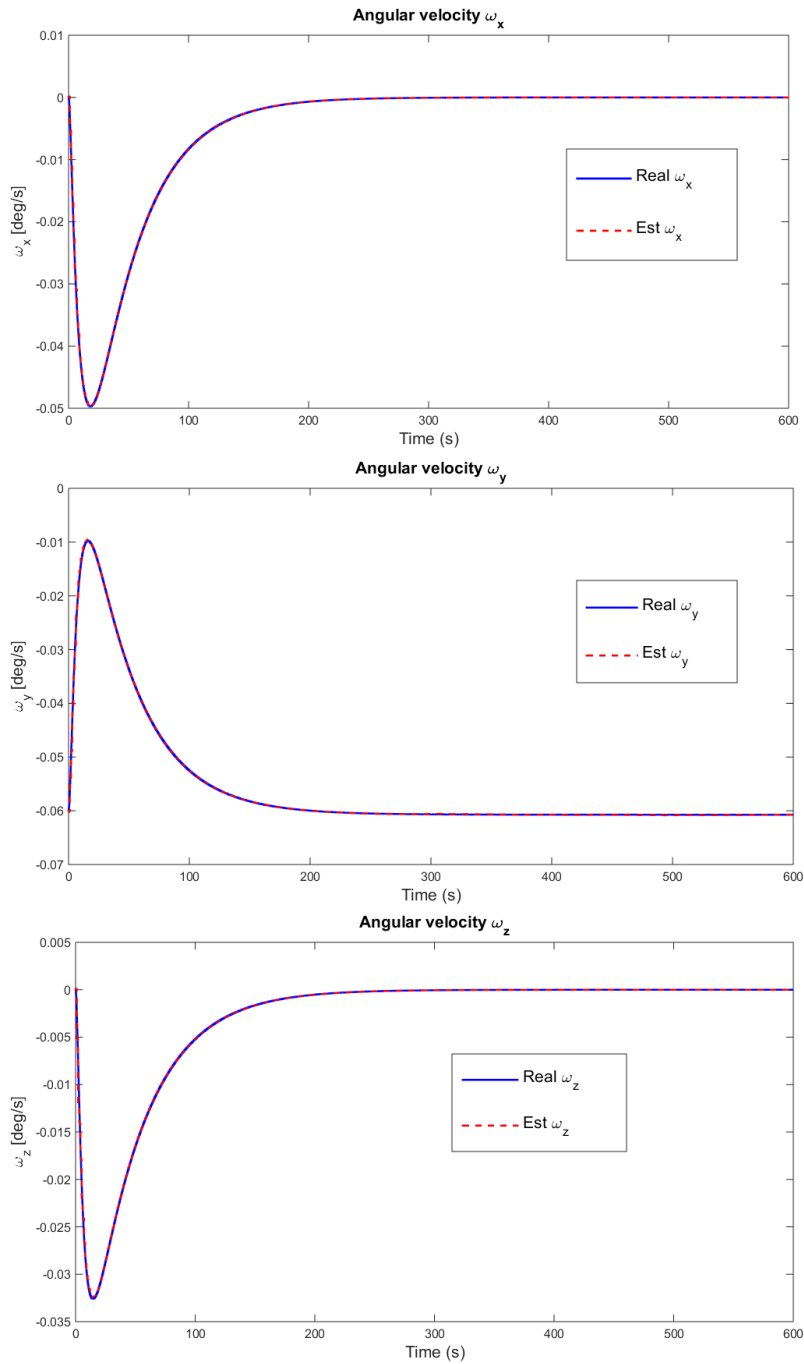


Fig. 1 Real and estimated angular velocity

EKF#1 and EKF#2, respectively.

As can be clearly seen from Table 3, the LSE#1 has an inertia estimation error about 2%.

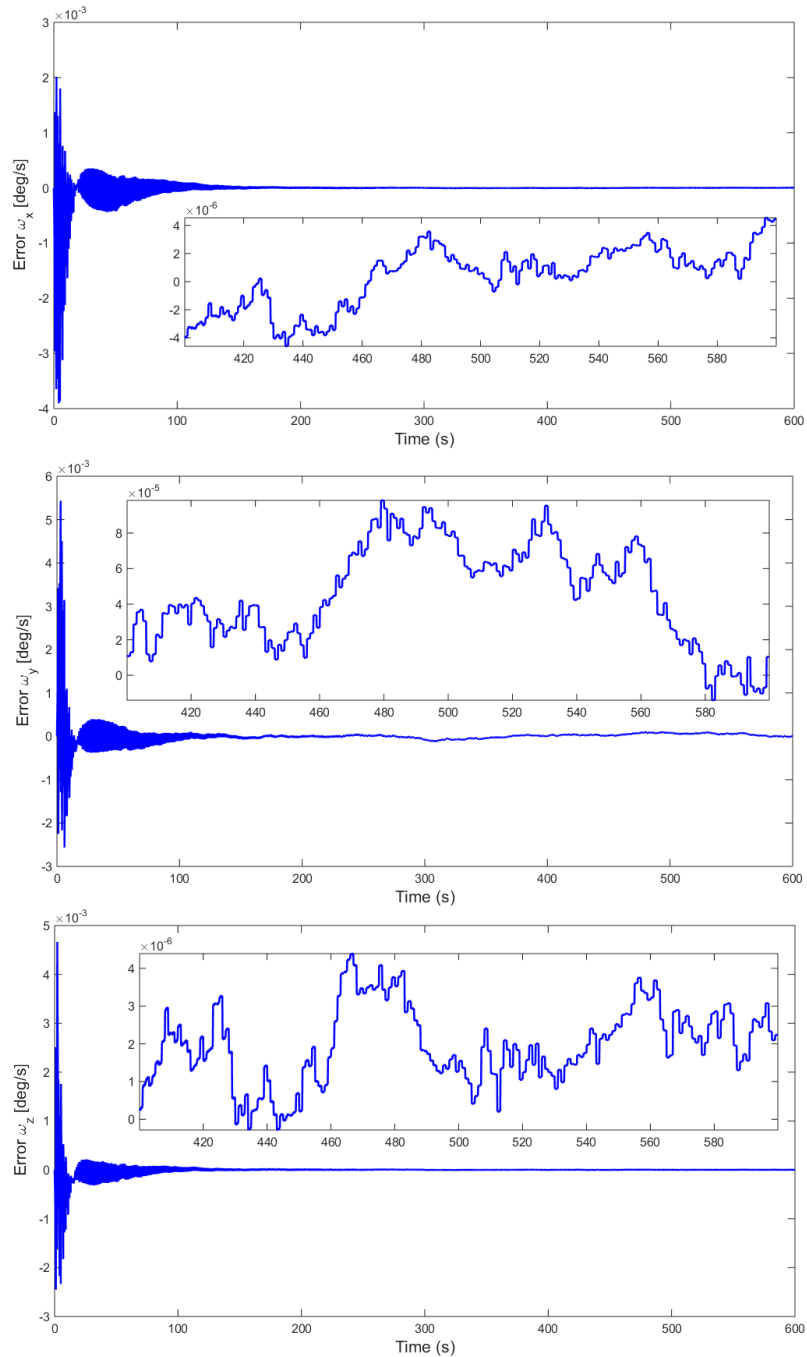


Fig. 2 Angular velocity estimation error

This filter produces a poorest accuracy compared with the adopted method in this work despite the use of three sensors (gyroscope, magnetometer and sun sensor). Otherwise, the results obtained with EKF#1 and EKF#2 give acceptable moment of inertia estimation with an error of 0.12%

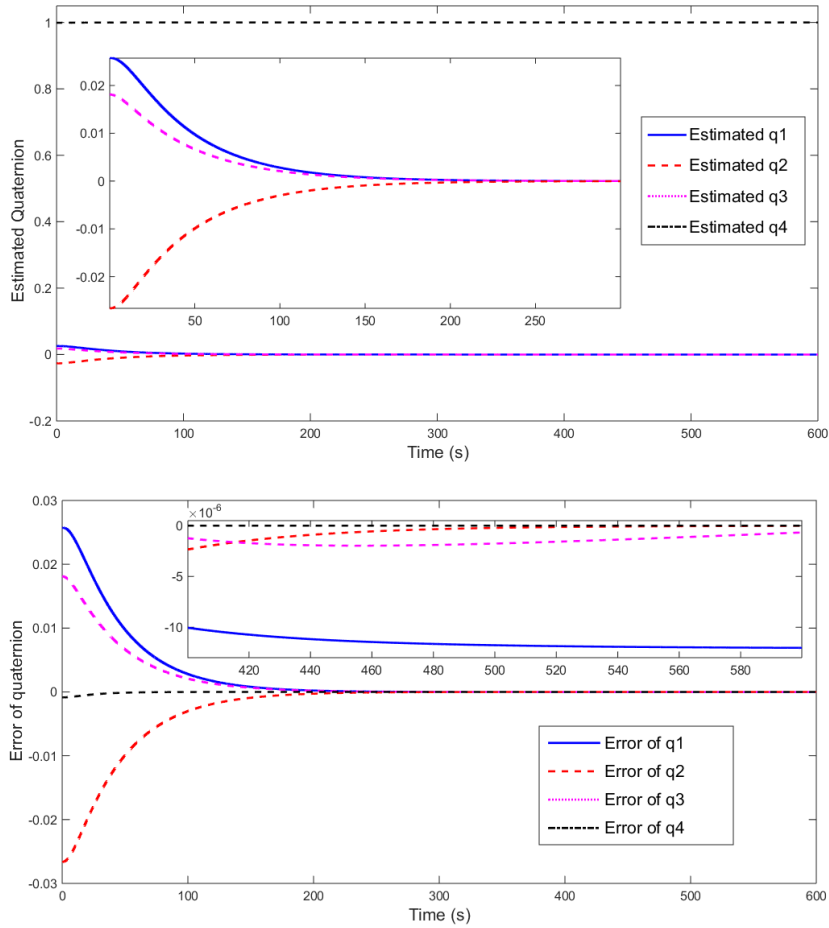


Fig. 3 Real and estimated quaternion and quaternion estimation error

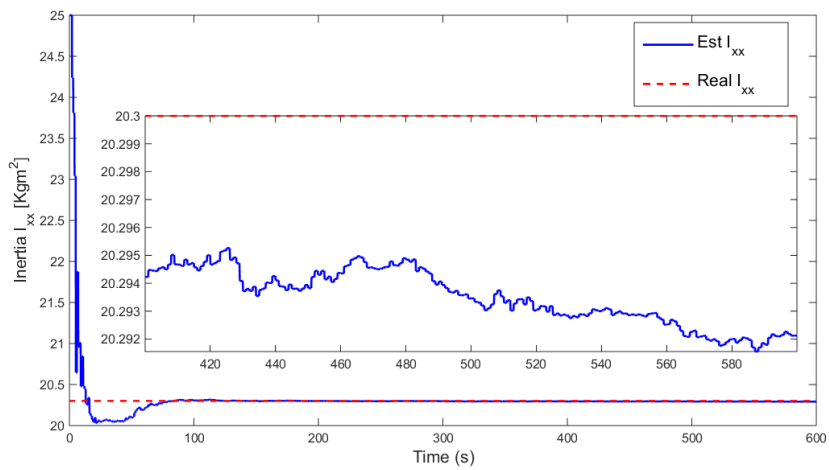


Fig. 4 Real and estimated moment of inertia

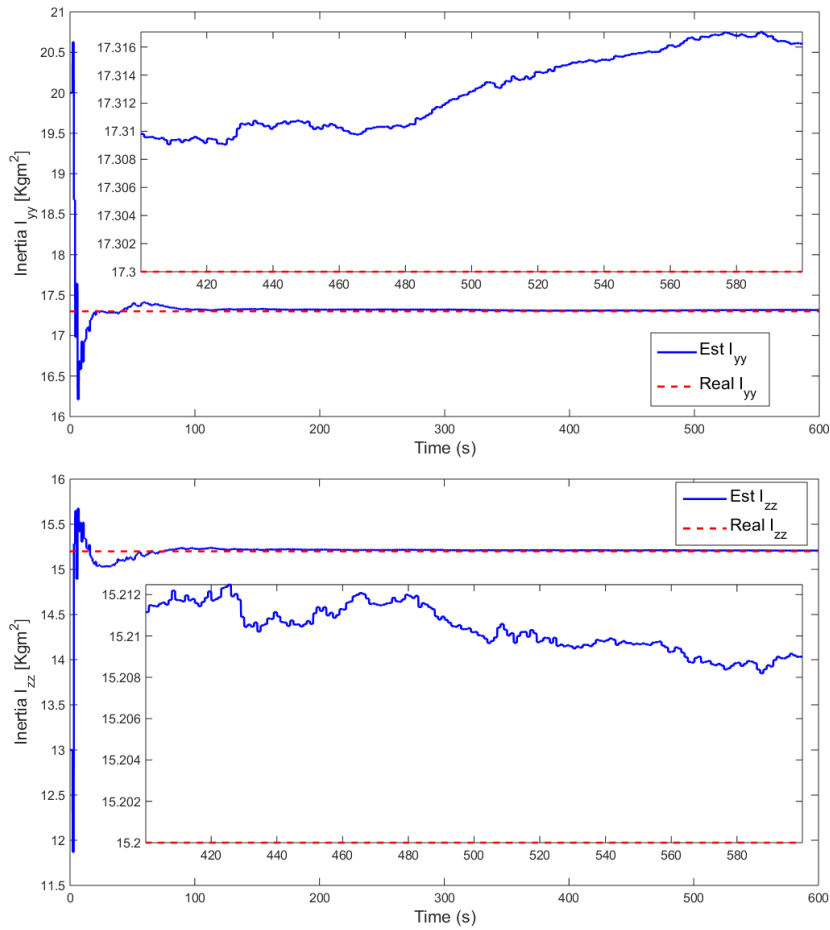


Fig. 4 Continued

and 0.06%, respectively. The both methods and the proposed method proved to meet the requirement satellite inertia tensor estimation with little difference in the accuracy obtained. However, a nominal inertia matrix is included in the EKF#1 algorithm, which has an unfavourable effect on the angular velocity estimation (Bellar and Mohammed 2019). In addition, the proposed algorithm estimates the full attitude of the satellite (quaternion and angular velocities) and without any application of constant magnitude control torques, applied in EKF#1 and EKF#2. This torque creates a tumbling attitude for the satellite and causes angular velocity divergence (see Fig. 5), which induces an unwanted behaviour and can lead to catastrophe in orbit. Therefore, this confirms the significant advantages of our proposed method, by ensuring better inertia estimation accuracy (around 0.09%) in nadir pointing mode.

The estimator capability is highlighted in Fig. 6, capturing the algorithm accuracy through a display of a histogram of MOI percent error for a Monte Carlo run 10000 times. In fact, the estimator converges for all over Monte Carlo runs and never diverges; moreover, the estimation error does not exceed 0.12% of the real inertia tensor, which confirms the performance of the filter within the interval of interest.

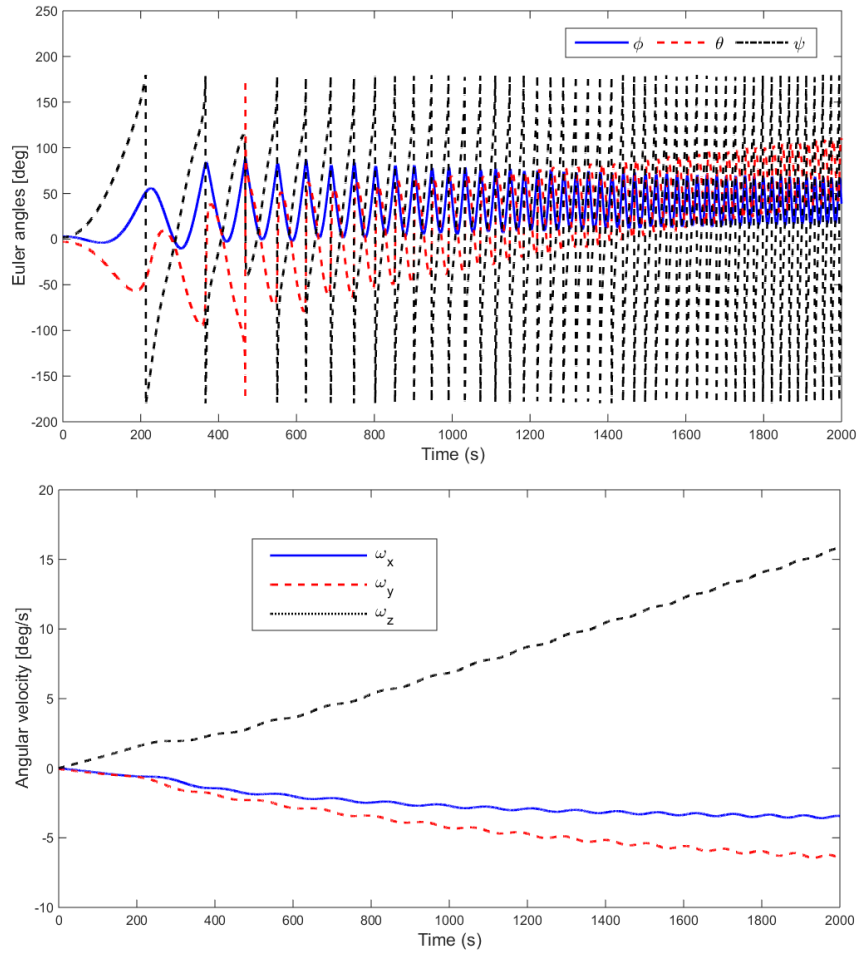


Fig. 5 Constant control torque effect on the attitude and angular velocity

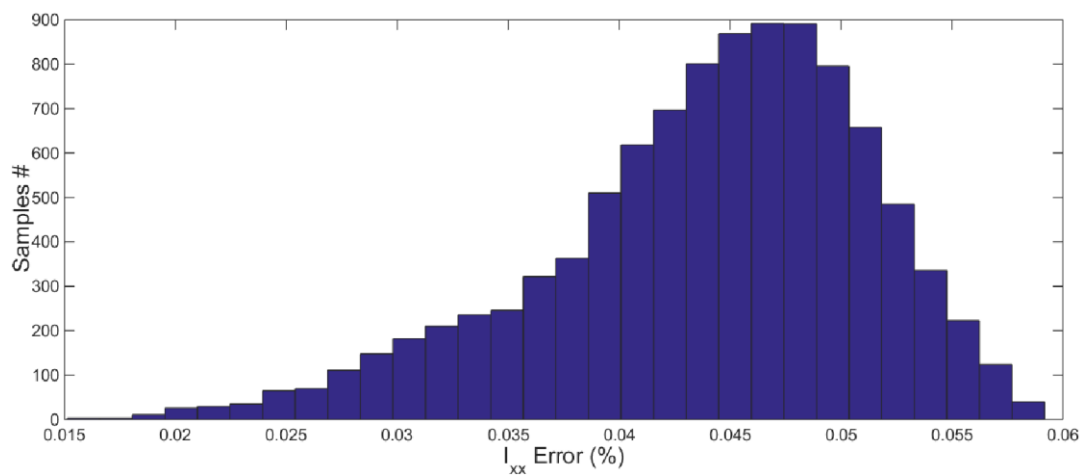


Fig. 6 Histogram of inertia tensor error (%) for 10000 Monte-Carlo runs

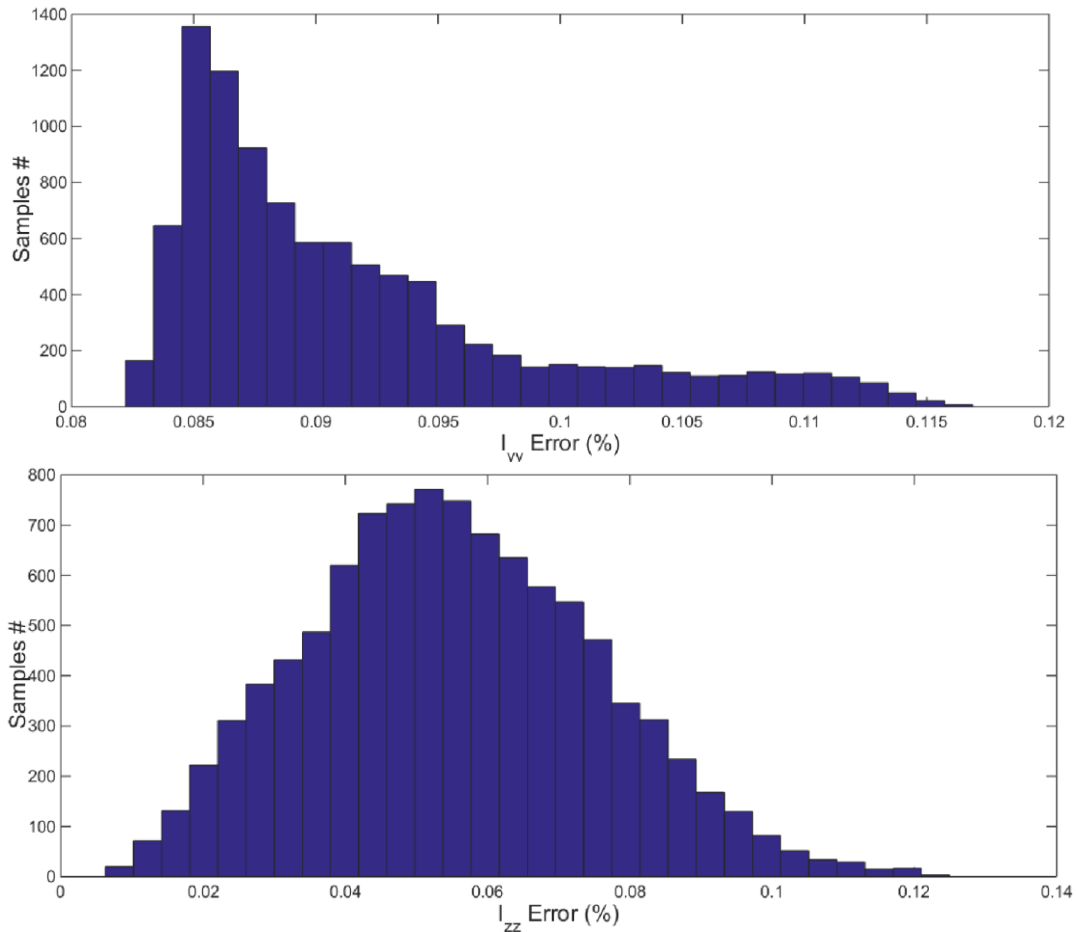


Fig. 6 Continued

4. Conclusions

This paper presented an estimation algorithm of attitude and inertia tensor. The proposed method consisted of an extended Kalman filter design based on star tracker data to obtain the quaternion, the angular velocity and the inertia parameters for a rigid nadir pointing microsatellite. The estimation approach drives its advantages from the fact that there is no use of nominal inertia and no application of constant control torque, which, at a time, reduce the impact of the inertia tensor error on the attitude estimation and avoid undesirable tumbling attitude. The simulation results, validated through Monte Carlo analysis, showed the efficiency of the proposed algorithm as well as the conformity and the accuracy of the attitude and the inertia tensor estimation.

Future works aim to develop a new hybrid navigation filter, which simultaneously estimates full attitude, inertia tensor and orbital parameters of the satellite.

References

Adnane, A., Foitih, Z.A., Mohammed, M.A.S. and Bellar, A. (2018), "Real-time sensor fault detection and

- isolation for LEO satellite attitude estimation through magnetometer data”, *Adv. Sp. Res.*, **61**(4), 1143-1157. <https://doi.org/10.1016/j.asr.2017.12.007>.
- Bellar, A. and Mohammed, M.A.S. (2019), “Satellite inertia parameters estimation based on extended Kalman Filter”, *J. Aerosp. Technol. Manage.*, **11**, 1-11. <https://doi.org/10.5028/jatm.v11.1016>.
- Bergmann, E. and Dzielski, J. (1990), “Spacecraft mass property identification with torque-generating control”, *J. Guid. Control Dynam.*, **13**(1), 99-103. <https://doi.org/10.2514/3.20522>.
- Bergmann, E.V., Walker, B.K. and Levy, D.R. (1987), “Mass property estimation for control of asymmetrical satellites”, *J. Guid. Control Dynam.*, **10**(5), 483-491. <https://doi.org/10.2514/3.20243>.
- Bordany, R., Steyn, W.H. and Crawford, M. (2000), “In-orbit estimation of the inertia matrix and thruster parameters of UoSAT-12”, *Proceedings of the 14th AIAA/USU Conference on Small Satellites*, Logan, U.S.A., August.
- Chashmi, S.Y.N. and Malaek, S.M.B. (2016), “Fast estimation of space-robots inertia parameters: A modular mathematical formulation”, *Acta Astronautica*, **127**, 283-295. <https://doi.org/10.1016/j.actaastro.2016.04.037>.
- Keim, J.A., Acikmese, A.B. and Shields, J.F. (2006), “Spacecraft inertia estimation via constrained least squares”, *Proceedings of the IEEE Aerospace Conference*, Big Sky, Montana, U.S.A., March.
- Kim, D., Yang, S. and Lee, S. (2016), “Rigid body inertia estimation using extended Kalman and Savitzky-Golay filters”, *Math. Probl. Eng.*, 1-7. <https://doi.org/10.1155/2016/2962671>.
- Kim, D.H., Yang, S., Cheon, D.I., Lee, S. and Oh, H.S. (2010), “Combined estimation method for inertia properties of STSAT-3”, *J. Mech. Sci. Technol.*, **24**(8), 1737-1741. <https://doi.org/10.1007/s12206-010-0521-2>.
- Kutlu, A., Hacıyev, C. and Tekinalp, O. (2007), “Attitude determination and rotational motion parameters identification of a LEO satellite through magnetometer and sun sensor data”, *Proceedings of the 3rd International Conference on Recent Advances in Space Technologies*, Istanbul, Turkey, June.
- Linares, R., Leve, F.A., Jan, M.K. and Crassidis, J.L. (2012), “Space object mass-specific inertia matrix estimation from photometric data”, *Adv. Astronaut. Sci.*, **144**, 41-54.
- Lorenzetti, J S., Bañuelos, L., Clarke, R., Murillo, O.J. and Bowers, A. (2017), “Determining products of inertia for small scale UAVs”, *Proceedings of the 55th AIAA Aerospace Sciences Meeting*, Grapevine, Texas, U.S.A., January.
- Manchester, Z. R. and Peck, M. A. (2017), “Recursive inertia estimation with semidefinite programming”, *Proceedings of the AIAA Guidance, Navigation, and Control Conference*, Grapevine, Texas, U.S.A., January.
- Muliadi, J., Langit, R. and Kusumoputro, B. (2017), “Estimating the UAV moments of inertia directly from its flight data”, *Proceedings of the 15th International Conference on Quality in Research (QiR): International Symposium on Electrical and Computer Engineering*, Nusa Dua, Indonesia, July.
- Ni, Z., Wu, Z., Liu, J. and Shen, X. (2017), “On-orbit identification of time-varying moment of inertia for spacecraft based on a recursive subspace method”, *Proceedings of the 36th Chinese Control Conference (CCC)*, Dalian, China, July.
- Palimaka, J. and Burlton, B. (1992), “Estimation of spacecraft mass properties using angular rate gyro data”, *Proceedings of the Guidance, Navigation and Control Conference*, Hilton Head Island, South Carolina, U.S.A., August.
- Salem, F.A. and Aly, A.A. (2015), “PD controller structures: Comparison and selection for an electromechanical system”, *Int. J. Intell. Syst. Appl.*, **7**(2), 1-12. <https://doi.org/10.5815/ijisa.2015.02.01>.
- Sidi, M.J. (1997), *Spacecraft Dynamics and Control: A Practical Engineering Approach*, Cambridge University Press, Cambridge, U.K.
- Tanygin, S. and Williams, T. (1997), “Mass property estimation using coasting maneuvers”, *J. Guid. Control Dynam.*, **20**(4), 625-632. <https://doi.org/10.2514/2.4099>.
- Thienel, J., Luquette, R. and Sanner, R. (2008), “Estimation of spacecraft inertia parameters”, *Proceedings of the AIAA Guidance, Navigation and Control Conference and Exhibit*, Honolulu, Hawaii, U.S.A., August.
- Wertz, J. R. (2012), *Spacecraft Attitude Determination and Control*, Springer Science and Business Media,

- Berlin, Germany.
- Wie, B., Weiss, H. and Arapostathis, A. (1989), "Quaternion feedback regulator for spacecraft eigenaxis rotations", *J. Guid. Control Dynam.*, **12**(3), 375-380. <https://doi.org/10.2514/3.20418>.
- Xu, B. and Wang, S. (2017), "Vision-based moment of inertia estimation of non-cooperative space object", *Proceedings of the 10th International Symposium on Computational Intelligence and Design (ISCID)*, Hangzhou, China, December.
- Yadegari, H., Khouane, B., Yukai, Z. and Chao, H. (2018), "Disturbance observer based anti-disturbance fault tolerant control for flexible satellites", *Adv. Aircraft Spacecraft Sci.*, **5**(4), 459-475. <https://doi.org/10.12989/aas.2018.5.4.459>.
- Yang, S., Lee, S., Lee, J.H. and Oh, H.S. (2015), "New real-time estimation method for inertia properties of STSAT-3 using gyro data", *T. Japan Soc. Aeronaut. Sp. Sci.*, **58**(4), 247-249. <https://doi.org/10.2322/tjsass.58.247>.
- Yang, Y. and Zhou, Z. (2017), "Attitude estimation: with or without spacecraft dynamics?", *Adv. Aircraft Spacecraft Sci.*, **4**(3), 335-351. <https://doi.org/10.12989/aas.2017.4.3.335>.
- Yoon, H., Riesing, K.M. and Cahoy, K. (2017), "Kalman filtering for attitude and parameter estimation of nanosatellites without gyroscopes", *J. Guid. Control Dynam.*, **40**(9), 2272-2288. <https://doi.org/10.2514/1.G002649>.
- Zhai, K., Wang, T. and Meng, D. (2017), "Optimal excitation design for identifying inertia parameters of spacecraft". *Acta Astronautica*, **140**, 370-379. <https://doi.org/10.1016/j.actaastro.2017.08.002>.
- Zhao, Y., Zhang, D., Tian, H. and Li, N. (2009), "Mass property estimation for mated flight control", *Proceedings of the International Conference on Computer Modeling and Simulation*, Macau, China, February.